2

Analysis of a Rectangular Microstrip Antenna on a Uniaxial Substrate

Amel Boufrioua
Electronics Department University of Constantine,
25000 Constantine,
Algeria

1. Introduction

Over the past years microstrip resonators have been widely used in the range of microwave frequencies. In general these structures are poor radiators, but by proper design the radiation performance can be improved and these structures can be used as antenna elements (Damiano & Papiernik, 1994). In recent years microstrip patch antennas became one of the most popular antenna types for use in aerospace vehicles, telemetry and satellite communication. These antennas consist of a radiating metallic patch on one side of a thin, non conducting, supporting substrate panel with a ground plane on the other side of the panel. For the analysis and the design of microstrip antennas there have been several techniques developed (Damiano & Papiernik, 1994; Mirshekar-Syahkal, 1990). The spectral domain approach is extensively used in microstrip analysis and design (Mirshekar-Syahkal, 1990). In such an approach, the spectral dyadic Green's function relates the tangential electric fields and currents at various conductor planes. It is found that the substrate permittivity is a very important factor to be determined in microstrip antenna designs. Moreover the study of anisotropic substrates is of interest, many practical substrates have a significant amount of anisotropy that can affect the performance of printed circuits and antennas, and thus accurate characterization and design must account for this effect (Bhartia et al. 1991). It is found that the use of such materials may have a beneficial effect on circuit or antenna (Bhartia et al. 1991; Pozar, 1987). For a rigorous solution to the problem of a rectangular microstrip antenna, which is the most widely used configuration because its shape readily allows theoretical analysis, Galerkin's method is employed in the spectral domain with two sets of patch current expansions. One set is based on the complete set of orthogonal modes of the magnetic cavity, and the other employs Chebyshev polynomials with the proper edge condition for the patch currents (Tulintsef et al. 1991).
This chapter describes spectral domain analyses of a rectangular microstrip patch antenna that contains isotropic or anisotropic substrates in which entire domain basis functions are used to model the patch current, we will present the effect of uniaxial anisotropy on the characterization of a rectangular microstrip patch antenna, also because there has been very little work on the scattering radar cross section of printed antennas in the literature, including the effect of a uniaxial anisotropic substrate, a number of results pertaining to this case will be presented in this chapter.

2. Theory

An accurate design of a rectangular patch antenna can be done by using the Galerkin procedure of the moment method (Pozar, 1987; Row & Wong, 1993; Wong et al., 1993). An integral equation can be formulated by using the Green's function on a thick dielectric substrate to determine the electric field at any point.

The patch is assumed to be located on a grounded dielectric slab of infinite extent, and the ground plane is assumed to be perfect electric conductor, the rectangular patch with length a and width b is embedded in a single substrate, which has a uniform thickness of h (see Fig. 1), all the dielectric materials are assumed to be nonmagnetic with permeability μ_0. To simplify the analysis, the antenna feed will not be considered.

The study of anisotropic substrates is of interest, however, the designers should, carefully check for the anisotropic effects in the substrate material with which they will work, and evaluate the effects of anisotropy.

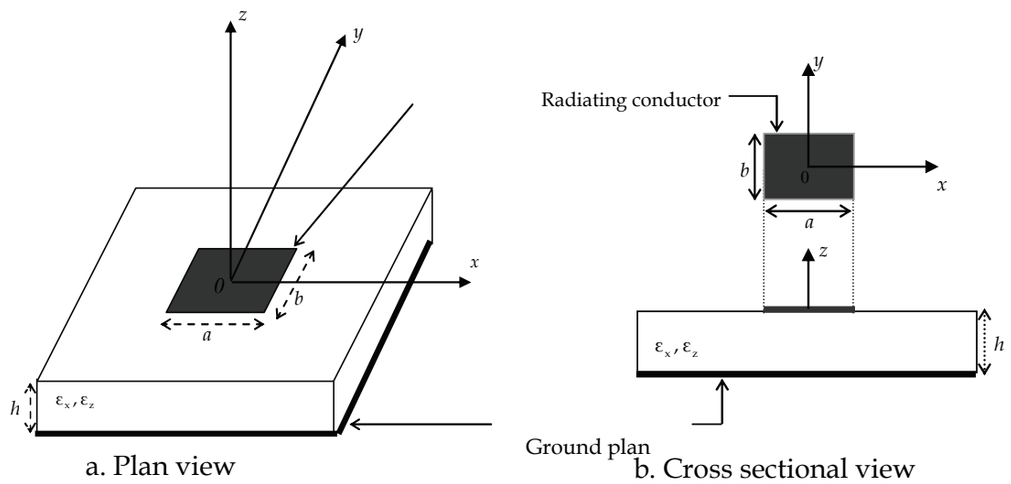

Fig. 1. Geometry of a rectangular microstrip antenna

Anisotropy is defined as the substrate dielectric constant on the orientation of the applied electric field. Mathematically, the permittivity of an anisotropic substrate can be represented by a tensor or dyadic of this form (Bhartia et al., 1991)

$$\boldsymbol{\varepsilon} = \varepsilon_0 \cdot \begin{bmatrix} \varepsilon_{xx} & \varepsilon_{xy} & \varepsilon_{xz} \\ \varepsilon_{yx} & \varepsilon_{yy} & \varepsilon_{yz} \\ \varepsilon_{zx} & \varepsilon_{zy} & \varepsilon_{zz} \end{bmatrix} \tag{1}$$

For a biaxially anisotropic substrate the permittivity is given by

$$\boldsymbol{\varepsilon} = \varepsilon_0 \cdot \begin{bmatrix} \varepsilon_x & 0 & 0 \\ 0 & \varepsilon_y & 0 \\ 0 & 0 & \varepsilon_z \end{bmatrix} \tag{2}$$

For a uniaxially anisotropic substrate the permittivity is

$$\boldsymbol{\varepsilon} = \varepsilon_0 \cdot \begin{bmatrix} \varepsilon_x & 0 & 0 \\ 0 & \varepsilon_x & 0 \\ 0 & 0 & \varepsilon_z \end{bmatrix} \tag{3}$$

ε_0 is the free-space permittivity.

ε_x is the relative permittivity in the direction perpendicular to the optical axis.

ε_z is the relative permittivity in the direction of the optical axis.

Many substrate materials used for printed circuit antenna exhibit dielectric anisotropy, especially uniaxial anisotropy (Bhartia et al. 1991; Wong et al., 1993).

In the following, the substrate material is taken to be isotropic or uniaxially anisotropic with the optical axis normal to the patch.

The boundary condition on the patch is given by (Pozar, 1987)

$$\mathbf{E}_{\text{scat}} + \mathbf{E}_{\text{inc}} = 0 \tag{4}$$

$\mathbf{E}_{\text{inc}}$ Tangential components of incident electric field.

$\mathbf{E}_{\text{scat}}$ Tangential components of scattered electric field.

While it is possible to work with wave equations and the longitudinal components $\tilde{\mathbf{E}}_z$ and $\tilde{\mathbf{H}}_z$, in the Fourier transform domain, it is desired to find the transverse fields in the (TM, TE) representation in terms of the longitudinal components. Assuming an $e^{i\omega t}$ time variation, thus Maxwells equations

$$\nabla \times \mathbf{H} = \varepsilon \frac{\partial \mathbf{E}}{\partial t} = i\,\omega\,\varepsilon\,\mathbf{E} \tag{5}$$

$$\nabla \times \mathbf{E} = \mu_0 \frac{\partial \mathbf{H}}{\partial t} = -i\,\omega\,\mu_0\,\mathbf{H} \tag{6}$$

Applying the divergence condition component

$$\nabla \cdot \mathbf{E} = \frac{\partial \mathbf{E}_x}{\partial x} + \frac{\partial \mathbf{E}_y}{\partial y} + \frac{\partial \mathbf{E}_z}{\partial z} = 0 \tag{7}$$

$$\nabla \cdot \mathbf{H} = \frac{\partial \mathbf{H}_x}{\partial x} + \frac{\partial \mathbf{H}_y}{\partial y} + \frac{\partial \mathbf{H}_z}{\partial z} = 0 \tag{8}$$

$i = \sqrt{-1}$

ω is the angular frequency.

From the above equations and after some algebraic manipulation, the wave equations for $\mathbf{E}_z$ and $\mathbf{H}_z$ are respectively

$$\frac{\partial^2 \mathbf{E}_z}{\partial x^2} + \frac{\partial^2 \mathbf{E}_z}{\partial y^2} + \frac{\varepsilon_x}{\varepsilon_z}\frac{\partial^2 \mathbf{E}_z}{\partial z^2} + \varepsilon_z\, k_0^2\, \mathbf{E}_z = 0 \tag{9}$$

$$\frac{\partial^2 \mathbf{H_z}}{\partial x^2}+\frac{\partial^2 \mathbf{H_z}}{\partial y^2}+\frac{\varepsilon_x}{\varepsilon_z}\frac{\partial^2 \mathbf{H_z}}{\partial z^2}+\varepsilon_z\, k_0^2\, \mathbf{H_z}=0 \tag{10}$$

With

k_0 propagation constant for free space, $k_0=\omega\sqrt{\varepsilon_0\,\mu_0}$

By assuming plane wave propagation of the form $e^{\pm i k_x x}\, e^{\pm i k_y y}\, e^{\pm i k_z z}$

A Fourier transform pair of the electric field is given by (Pozar, 1987)

$$\tilde{\mathbf{E}}(k_x,k_y,k_z)=\iint_{-\infty}\mathbf{E}(x,y,z)\,e^{-ik_x x}\,e^{-ik_y y}\,dx\,dy \tag{11}$$

$$\mathbf{E}(x,y,z)=\frac{1}{4\pi^2}\iint_{-\infty}\tilde{\mathbf{E}}(k_x,k_y,k_z)\,e^{ik_x x}\,e^{ik_y y}\,dk_x\,dk_y \tag{12}$$

A Fourier transform pair of the magnetic field is given by (Pozar, 1987)

$$\tilde{\mathbf{H}}(k_x,k_y,k_z)=\iint_{-\infty}\mathbf{H}(x,y,z)\,e^{-ik_x x}\,e^{-ik_y y}\,dx\,dy \tag{13}$$

$$\mathbf{H}(x,y,z)=\frac{1}{4\pi^2}\iint_{-\infty}\tilde{\mathbf{H}}(k_x,k_y,k_z)\,e^{ik_x x}\,e^{ik_y y}\,dk_x\,dk_y \tag{14}$$

It is worth noting that ~ is used to indicate the quantities in spectral domain.

In the spectral domain $\frac{\partial}{\partial x}=i\,k_x$, $\frac{\partial}{\partial y}=i\,k_y$, $\frac{\partial}{\partial z}=i\,k_z$ and $\frac{\partial}{\partial t}=i\,\omega\,t$

After some straightforward algebraic manipulation the transverse field can be written in terms of the longitudinal components $\tilde{\mathbf{E}}_z$, $\tilde{\mathbf{H}}_z$

$$\tilde{\mathbf{E}}_x=\frac{i\,\varepsilon_z\,k_x}{\varepsilon_x\,\mathbf{k_s^2}}\frac{\partial\tilde{\mathbf{E}}_z}{\partial z}+\frac{\omega\,\mu_0\,k_y}{\mathbf{k_s^2}}\tilde{\mathbf{H}}_z \tag{15}$$

$$\tilde{\mathbf{E}}_y=\frac{i\,\varepsilon_z\,k_y}{\varepsilon_x\,\mathbf{k_s^2}}\frac{\partial\tilde{\mathbf{E}}_z}{\partial z}-\frac{\omega\,\mu_0\,k_x}{\mathbf{k_s^2}}\tilde{\mathbf{H}}_z \tag{16}$$

$$\tilde{\mathbf{H}}_x=-\frac{\omega\,\varepsilon_z\varepsilon_0\,k_y}{\mathbf{k_s^2}}\tilde{\mathbf{E}}_z+\frac{i\,k_x}{\mathbf{k_s^2}}\frac{\partial\tilde{\mathbf{H}}_z}{\partial z} \tag{17}$$

$$\tilde{\mathbf{H}}_y=-\frac{\omega\,\varepsilon_z\varepsilon_0\,k_x}{\mathbf{k_s^2}}\tilde{\mathbf{E}}_z+\frac{i\,k_y}{\mathbf{k_s^2}}\frac{\partial\tilde{\mathbf{H}}_z}{\partial z} \tag{18}$$

$\mathbf{k_s}$ is the transverse wave vector, $\mathbf{k_s}=k_x\hat{\mathbf{x}}+k_y\hat{\mathbf{y}}$, $k_s=|\mathbf{k_s}|$

k_x and k_y are the spectral variables corresponding to x and y respectively.

From the wave equations (9) and (10), the general form of $\tilde{\mathbf{E}}_z$ and $\tilde{\mathbf{H}}_z$ is

$$\tilde{\mathbf{E}}_z = \mathbf{C_1}\, e^{-ik_z z} + \mathbf{D_1}\, e^{ik_z z} \tag{19}$$

$$\tilde{\mathbf{H}}_z = \mathbf{C_2}\, e^{-ik_z z} + \mathbf{D_2}\, e^{ik_z z} \tag{20}$$

$\mathbf{C_1}$, $\mathbf{D_1}$, $\mathbf{C_2}$ and $\mathbf{D_2}$ are the unknowns to be determined.
By substitution of (19) and (20) in (15)-(18) and after some algebraic manipulation the transverse field in the (TM, TE) representation can be written by

$$\tilde{\mathbf{E}}_s(\mathbf{k}_s, z) = \begin{bmatrix} \tilde{\mathbf{E}}_s^{\,e}(\mathbf{k}_s, z) \\ \tilde{\mathbf{E}}_s^{\,h}(\mathbf{k}_s, z) \end{bmatrix} = e^{ik_z z}\, \mathbf{A}(k_s) + e^{-ik_z z}\, \mathbf{B}(\mathbf{k}_s) \tag{21}$$

$$\tilde{\mathbf{H}}_s(\mathbf{k}_s, z) = \begin{bmatrix} \tilde{\mathbf{H}}_s^{\,e}(\mathbf{k}_s, z) \\ \tilde{\mathbf{H}}_s^{\,h}(\mathbf{k}_s, z) \end{bmatrix} = \mathbf{g}(\mathbf{k}_s)\left[e^{ik_z z}\, \mathbf{A}(\mathbf{k}_s) - e^{-ik_z z}\, \mathbf{B}(\mathbf{k}_s)\right] \tag{22}$$

The superscripts e and h denote the TM and the TE waves, respectively.
A and **B** are two unknowns vectors to be determined, note that are expressed in terms of $\mathbf{C_1}$, $\mathbf{D_1}$, $\mathbf{C_2}$ and $\mathbf{D_2}$.
Where

$$\mathbf{g}(\mathbf{k}_s) = \begin{bmatrix} \dfrac{\omega \varepsilon_0 \varepsilon_x}{k_z^e} & 0 \\ 0 & \dfrac{k_z^h}{\omega \mu_0} \end{bmatrix} \tag{23}$$

$$\mathbf{k_z} = \begin{bmatrix} k_z^e & 0 \\ 0 & k_z^h \end{bmatrix},\ k_z^e = \left(\varepsilon_x k_0^2 - \frac{\varepsilon_x}{\varepsilon_z} k_s^2\right)^{\frac{1}{2}} \text{ and } k_z^h = \left(\varepsilon_x k_0^2 - k_s^2\right)^{\frac{1}{2}}$$

k_z^e and k_z^h are respectively propagation constants for TM and TE waves in the uniaxial dielectric.
By eliminating the unknowns **A** and **B**, in the equations (21) and (22) we obtain the following matrix which combines the tangential field components on both sides z1 and z2 of the considered layer as input and output quantities

$$\begin{bmatrix} \tilde{\mathbf{E}}^{e(h)}(\mathbf{k}_s, z_2^-) \\ \tilde{\mathbf{H}}^{e(h)}(\mathbf{k}_s, z_2^-) \end{bmatrix} = \begin{bmatrix} \mathbf{I}\cos(k_z^{e(h)} h) & i\mathbf{g}^{-1}\sin(k_z^{e(h)} h) \\ i\mathbf{g}\sin(k_z^{e(h)} h) & \mathbf{I}\cos(k_z^{e(h)} h) \end{bmatrix} \times \begin{bmatrix} \tilde{\mathbf{E}}^{e(h)}(\mathbf{k}_s, z_1^+) \\ \tilde{\mathbf{H}}^{e(h)}(\mathbf{k}_s, z_1^+) \end{bmatrix} - \begin{bmatrix} 0 \\ \tilde{\mathbf{J}}^{e(h)}(\mathbf{k}_s) \end{bmatrix} \tag{24}$$

I is the unit matrix.
$\tilde{\mathbf{J}}^{e(h)}(\mathbf{k}_s)$ is the current on the patch.
In the spectral domain the relationship between the patch current and the electric field on the patch is given by

$$\tilde{\mathbf{E}}_s(\mathbf{k}_s) = \mathbf{G}(\mathbf{k}_s) \cdot \tilde{\mathbf{J}}(\mathbf{k}_s) \tag{25}$$

G is the spectral dyadic Green's function

$$\mathbf{G}=\begin{bmatrix}\mathbf{G}^{e} & 0\\ 0 & \mathbf{G}^{h}\end{bmatrix} \tag{26}$$

$\mathbf{G}^{e}, \mathbf{G}^{h}$ are given by

$$\mathbf{G}^{e}=\frac{1}{i\omega\varepsilon_0}\frac{-k_z^{e}k_z\sin(k_{z1}h)}{ik_z^{e}\sin(k_{z1}h)+\varepsilon_x k_z\cos(k_{z1}h)} \tag{26a}$$

$$\mathbf{G}^{h}=\frac{1}{i\omega\varepsilon_0}\frac{-k_0^{2}\sin(k_{z1}h)}{ik_z\sin(k_{z1}h)+k_z^{h}\cos(k_{z1}h)} \tag{26b}$$

In the case of the isotroipc substrate

$$\mathbf{G}^{e}=\sqrt{\frac{\mu_0}{\varepsilon_0}}\frac{\cos(k_{z1}h)}{(1-i\varepsilon_r k_z\cot(k_{z1}h)/k_{z1})} \tag{26c}$$

$$\mathbf{G}^{h}=\sqrt{\frac{\mu_0}{\varepsilon_0}}\frac{1}{\cos(k_{z1}h)(1-i k_{z1}\cot(k_{z1}h)/k_z)} \tag{26d}$$

Where

$k_{z1}=k_0\cos(k_z h)$ and $k_z=(k_0^2-k_s^2)^{1/2}$

$\tilde{\mathbf{J}}(\mathbf{k}_s)$ is the current on the patch which related to the vector Fourier transform of $J(r_s)$, as (Chew & Liu, 1988)

$$\tilde{\mathbf{J}}(\mathbf{k}_s)=\int_{-\infty}^{\infty}\int d\mathbf{k}_s\mathbf{F}(\mathbf{k}_s,-\mathbf{r}_s)\cdot\mathbf{J}(\mathbf{r}_s) \tag{27}$$

Where

$$\mathbf{F}(\mathbf{k}_s,\mathbf{r}_s)=\frac{1}{k_s}\begin{bmatrix}k_x & k_y\\ k_y & -k_x\end{bmatrix}e^{i\mathbf{k}_s\cdot\mathbf{r}_s},\ \mathbf{r}_s=x\hat{\mathbf{x}}+y\hat{\mathbf{y}} \tag{28}$$

$\hat{\mathbf{x}}$ unit vector in x direction.

$\hat{\mathbf{y}}$ unit vector in y direction.

The surface current on the patch can be expanded into a series of known basis functions J_{xn} and J_{ym}

$$\mathbf{J}(\mathbf{r}_s)=\sum_{n=1}^{N}a_n\begin{bmatrix}J_{xn}(\mathbf{r}_s)\\ 0\end{bmatrix}+\sum_{m=1}^{M}b_m\begin{bmatrix}0\\ J_{ym}(\mathbf{r}_s)\end{bmatrix} \tag{29}$$

Where a_n and b_m are the unknown coefficients to be determined in the x and y direction respectively.

The latter expression is substituted into equation (27); the results can be given by

$$\tilde{\mathbf{J}}(\mathbf{k}_s)=\frac{1}{\mathbf{k}_s}\begin{bmatrix}k_x\\ k_y\end{bmatrix}\sum_{n=1}^{N}a_n\,\tilde{\mathbf{J}}_{xn}(\mathbf{k}_s)+\frac{1}{\mathbf{k}_s}\begin{bmatrix}k_y\\ -k_x\end{bmatrix}\sum_{m=1}^{M}b_m\,\tilde{\mathbf{J}}_{ym}(\mathbf{k}_s) \tag{30}$$

$\tilde{\mathbf{J}}_{xn}(\mathbf{k_s})$ and $\tilde{\mathbf{J}}_{ym}(\mathbf{k_s})$ are the Fourier transforms of $\mathbf{J}_{xn}(\mathbf{r_s})$ and $\mathbf{J}_{ym}(\mathbf{r_s})$ respectively.

One of the main problems with the computational procedure is to overcome the complicated time-consuming task of calculating the Green's functions in the procedure of resolution by the moment method. The choice of the basis function is very important for a rapid convergence to the true values (Boufrioua & Benghalia, 2008; Boufrioua, 2009).

Many subsequent analyses involve entire-domain basis functions that are limited to canonical shapes such as rectangles, circles and ellipses. Recently, much work has been published regarding the scattering properties of microstrip antennas on various types of substrate geometries. Virtually all this work has been done with entire domain basis functions for the current on the patch.

For the resonant patch, entire domain expansion currents lead to fast convergence and can be related to a cavity model type of interpretation (Boufrioua, 2009; Pozar & Voda, 1987). The currents can be defined using a sinusoid basis functions defined on the whole domain, without the edge condition (Newman & Forrai, 1987; Row & Wong, 1993), these currents associated with the complete orthogonal modes of the magnetic cavity. Both x and y directed currents were used, with the following forms (Chew & Liu, 1988; Row & Wong, 1993)

$$\mathbf{J}_{xn}(\mathbf{r_s}) = \sin\left[\frac{n_1\,\pi}{a}\left(x+\frac{a}{2}\right)\right]\cos\left[\frac{n_2\,\pi}{b}\left(y+\frac{b}{2}\right)\right] \tag{31a}$$

$$\mathbf{J}_{ym}(\mathbf{r_s}) = \cos\left[\frac{m_1\,\pi}{a}\left(x+\frac{a}{2}\right)\right]\sin\left[\frac{m_2\,\pi}{b}\left(y+\frac{b}{2}\right)\right] \tag{31b}$$

The Fourier transforms of J_{xn} and J_{ym} are obtained from equation (27) and given by

$$\tilde{\mathbf{J}}_{xn}(\mathbf{k_s}) = \int_{-a/2}^{a/2} dx\, e^{-ik_x x}\sin\left(\frac{n_1\pi}{a}\left(x+\frac{a}{2}\right)\right)\times\int_{-b/2}^{b/2} dy\, e^{-ik_y y}\cos\left(\frac{n_2\pi}{b}\left(y+\frac{b}{2}\right)\right) \tag{32a}$$

$$\tilde{\mathbf{J}}_{ym}(\mathbf{k_s}) = \int_{-a/2}^{a/2} dx\, e^{-ik_x x}\cos\left(\frac{m_1\pi}{a}\left(x+\frac{a}{2}\right)\right)\times\int_{-b/2}^{b/2} dy\, e^{-ik_y y}\sin\left(\frac{m_2\pi}{b}\left(y+\frac{b}{2}\right)\right) \tag{32b}$$

Since the chosen basis functions approximate the current on the patch very well for conventional microstrips, only one or two basis functions are used for each current component.

Using the equations (32.a) and (32.b), the integral equation describing the field **E** in the patch can be discretized into the following matrix

$$\begin{bmatrix}(\mathbf{Z}_1)_{N\times N} & (\mathbf{Z}_2)_{N\times M}\\ (\mathbf{Z}_3)_{M\times N} & (\mathbf{Z}_4)_{M\times M}\end{bmatrix}\cdot\begin{bmatrix}(\mathbf{a})_{N\times 1}\\ (\mathbf{b})_{M\times 1}\end{bmatrix} = 0 \tag{33}$$

Where the impedance matrix terms are

$$(\mathbf{Z}_1)_{kn} = \int_{-\infty}^{\infty}\int d\mathbf{k_s}\,\frac{1}{k_s^2}\left[k_x^2\mathbf{G}^e + k_y^2\mathbf{G}^h\right]\times\tilde{\mathbf{J}}_{xk}(-\mathbf{k_s})\,\tilde{\mathbf{J}}_{xn}(\mathbf{k_s}). \tag{34a}$$

$$(\mathbf{Z}_2)_{km} = \int_{-\infty}^{\infty}\int d\mathbf{k}_s \frac{k_x k_y}{k_s^2}\left[\mathbf{G}^e - \mathbf{G}^h\right]\times \tilde{\mathbf{J}}_{xk}(-\mathbf{k}_s)\tilde{\mathbf{J}}_{ym}(\mathbf{k}_s) \tag{34b}$$

$$(\mathbf{Z}_3)_{ln} = \int_{-\infty}^{\infty}\int d\mathbf{k}_s \frac{k_x k_y}{k_s^2}\left[\mathbf{G}^e - \mathbf{G}^h\right]\times \tilde{\mathbf{J}}_{yl}(-\mathbf{k}_s)\tilde{\mathbf{J}}_{xn}(\mathbf{k}_s) \tag{34c}$$

$$(\mathbf{Z}_4)_{lm} = \int_{-\infty}^{\infty}\int d\mathbf{k}_s \frac{1}{k_s^2}\left[k_y^2\mathbf{G}^e + k_x^2\mathbf{G}^h\right]\cdot \tilde{\mathbf{J}}_{yl}(-\mathbf{k}_s)\tilde{\mathbf{J}}_{ym}(\mathbf{k}_s) \tag{34d}$$

$\begin{bmatrix}(\mathbf{a})_{N\times 1}\\(\mathbf{b})_{M\times 1}\end{bmatrix}$ are the unknown current modes on the patch

It should be noted that the roots of the characteristic equation given by (33) are complex, Muller's algorithm has been employed to compute the roots and hence to determine the resonant frequency.

The integration of the matrix elements in equations (34) must be done numerically, but can be simplified by conversion from the (k_x, k_y) coordinates to the polar coordinates (k_ρ, α) with the following change.

$$\int_{-\infty}^{\infty}\int dk_s = \int_{-\infty}^{\infty}\int_{-\infty}^{\infty} dk_x\, dk_y = \int_0^{\infty} dk_\rho\, k_\rho \int_0^{2\pi} d\alpha \tag{35}$$

3. Antenna characteristics

Since the resonant frequencies are defined to be the frequencies at which the field and the current can sustain themselves without a driving source. Therefore, for the existence of nontrivial solutions, the determinant of the [z] matrix must be zero, i.e

$$\det(\mathbf{Z}(\omega)) = 0 \tag{36}$$

This condition is satisfied by a complex frequency $f = f_r + i\, f_i$ that gives the resonant frequency f_r, the half power bandwidth $BW = 2f_i/f_r$ and the other antenna characteristics.

Stationary phase evaluation yields convenient and useful results for the calculation of antenna patterns or radar cross section (Pozar, 1987).

The scattered far-zone electric field from the patch can then be found in spherical coordinates with components $\mathbf{E}_\theta$ and $\mathbf{E}_\phi$ and the results are of the form

$$\begin{bmatrix}\mathbf{E}_\theta\\ \mathbf{E}_\varphi\end{bmatrix} = i\, k_0 \frac{\exp(i\, k_0\, r)}{2\pi\, r}\begin{bmatrix}-\mathbf{G}^e & 0\\ 0 & \mathbf{G}^h\cos\theta\end{bmatrix}\begin{bmatrix}\tilde{\mathbf{J}}^e\\ \tilde{\mathbf{J}}^h\end{bmatrix} \tag{37}$$

In the above equation, k_x and k_y are evaluated at the stationary phase point as

$$k_x = k_0 \sin\theta\cos\varphi \tag{38a}$$

$$k_y = k_0 \sin\theta\sin\varphi \tag{38b}$$

The radar cross section of a microstrip patch has recently been treated (Knott et al., 2004), although, there has been very little work on the radar cross section of patch antennas in the

literature. The solution of the electric field integral equation via the method of moments has been a very useful tool for accurately predicting the radar cross section of arbitrarily shaped in the frequency domain (Reddy et al., 1998). In this chapter we will considere only monostatic scattering. The radar cross section computed from (Knott et al., 2004; Reddy et al., 1998), for a unit amplitude incident electric field the typical scattering results are of the form

$$\sigma_{\theta\theta} = 4\,\pi\, r^2 \left| E_{\theta}^{scat} \right|^2 \tag{39}$$

$\sigma_{\theta\theta}$ is $\hat{\theta}$-polarized backscatter from a unit amplitude $\hat{\theta}$ polarized incident field

$$RCS = 10 \log_{10}(\sigma_{\theta\theta}) \tag{40}$$

RCS is the radar cross section.

Computer programs have been written to evaluate the elements of the impedance matrix and then to solve the matrix equation. In Figure 2, comparisons are shown for the calculated and measured data presented by W. C. Chew and Q. Liu, deduced from table. I (Chew & Liu, 1988) and the calculated results from our model, for a perfectly conducting patches of different dimensions *a*(cm)×*b*(cm), without dielectric substrates (air) with thickness of 0.317cm. It is important to note that the normalization is with respect to f_0 of the magnetic wall cavity, the mode studied in this work is the dominant mode TM01. Our calculated results agree very well with experimental results, the maximum difference between the experimental and numerical results is less than 7%, this shift may indicate physical tolerances of the patch size or substrate dielectric parameters.

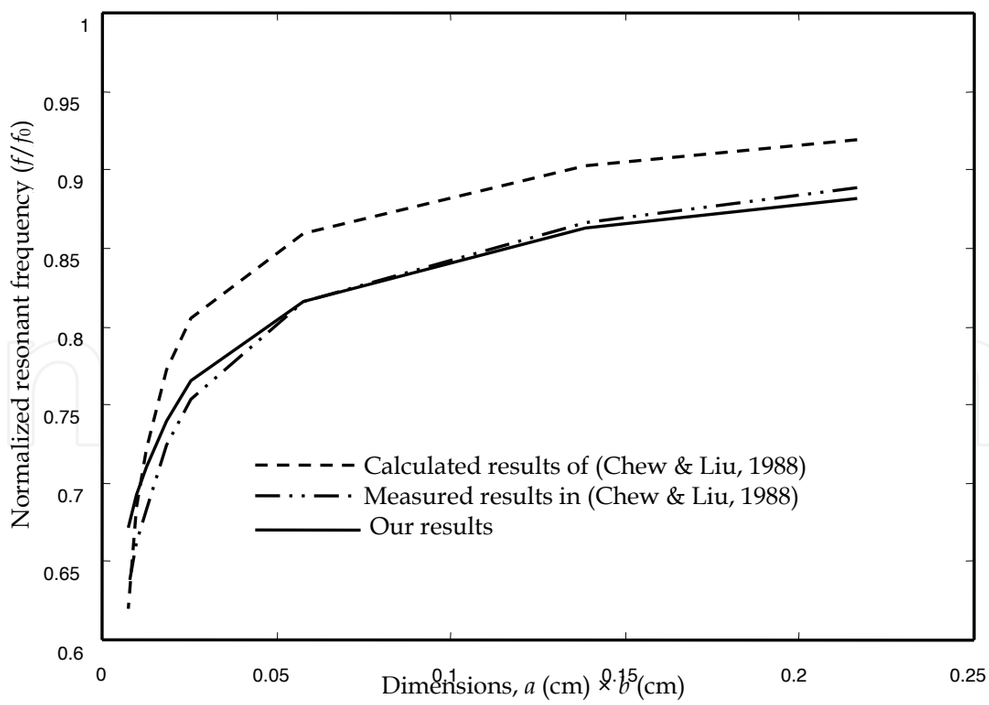

Fig. 2. Comparison between our calculated resonant frequencies and measured results versus the dimensions of the patch.

The influence of uniaxial anisotropy in the substrate on the resonant frequency, the quality factor and the half power band width of a rectangular microstrip patch antenna with dimensions *a*=1.5cm, *b*=1.0cm and the substrate has a thickness *h*=0.159 cm, for different pairs of relative permittivity (ε_x, ε_z) is shown in Table 1. The obtained results show that the positive uniaxial anisotropy slightly increases the resonant frequency and the half power band width, while the negative uniaxial anisotropy slightly decreases both the half power band width and the resonant frequency.

Comparisons are shown in table 2 for the calculated data presented by (Bouttout et al., 1999) and our calculated results for a rectangular patch antenna with dimensions *a*=1.9cm, *b*=2.29 cm and the substrate has a thickness *h*=0.159cm. The obtained results show that when the permittivity along the optical axis ε_z is changed and ε_x remains constant the resonant frequency changes drastically, on the other hand, we found a slight shift in the resonant frequency when the permittivity ε_x is changed and ε_z remains constant, these behaviors agree very well with those obtained by (Bouttout et al., 1999).

Uniaxial anisotropy type	Relative permittivity ε_x	Relative permittivity ε_z	Resonant frequency Ghz	Band width BW %	Quality factor Q
isotropic	2.35	2.35	8.6360194	9.0536891	11.0452213
isotropic	7.0	7.0	5.2253631	3.1806887	31.4397311
positive	1.88	2.35	8.7241626	9.1377564	10.9436053
negative	2.82	2.35	8.5537694	8.9779555	11.1383933
negative	8.4	7.0	5.1688307	3.1550166	31.6955535
positive	5.6	7.0	5.2869433	3.2124019	31.1293545

Table 1. Resonant frequency, band width and quality factor for the isotropic, positive and negative uniaxial anisotropic substrates

ε_x	ε_z	AR	Resonant frequencies (Ghz)	
			(Bouttout et al., 1999)	Our results
2.32	2.32	1	4.123	4.121
4.64	2.32	2	4.042	4.041
2.32	1.16	2	5.476	6.451
1.16	2.32	0.5	4.174	4.171
2.32	4.64	0.5	3.032	3.028

Table 2. Dependence of resonant frequency on relative permittivity (ε_x , ε_z)

The anisortopic ratio $AR = \varepsilon_x / \varepsilon_z$

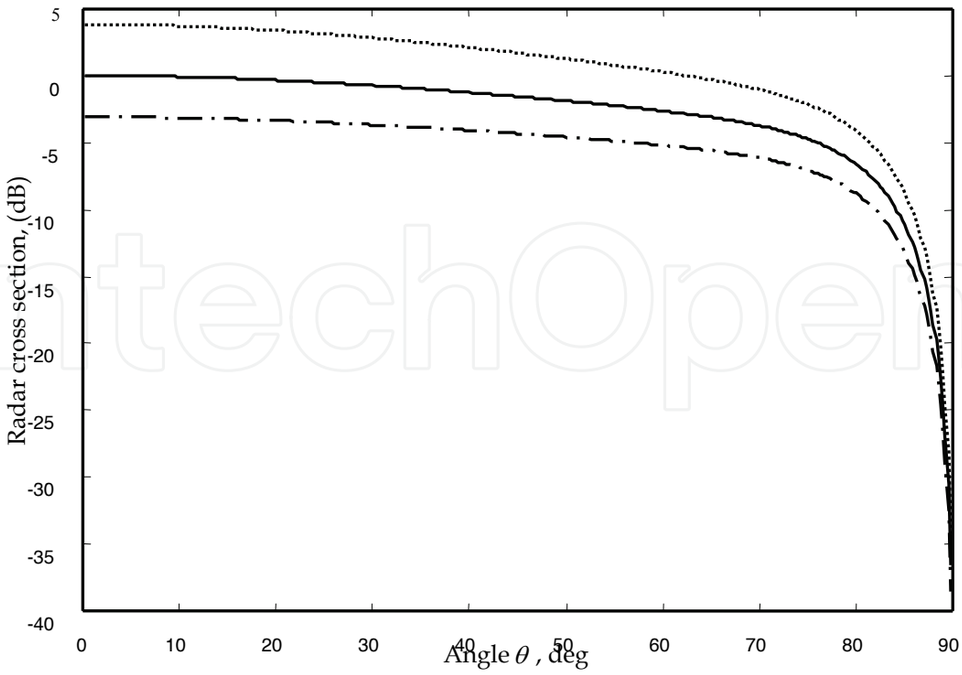

(a) ε_z changed, ——— $\varepsilon_x = \varepsilon_z = 5$, — · — · $\varepsilon_x = 5$, $\varepsilon_z = 6.4$, ····· $\varepsilon_x = 5$, $\varepsilon_z = 3.6$.

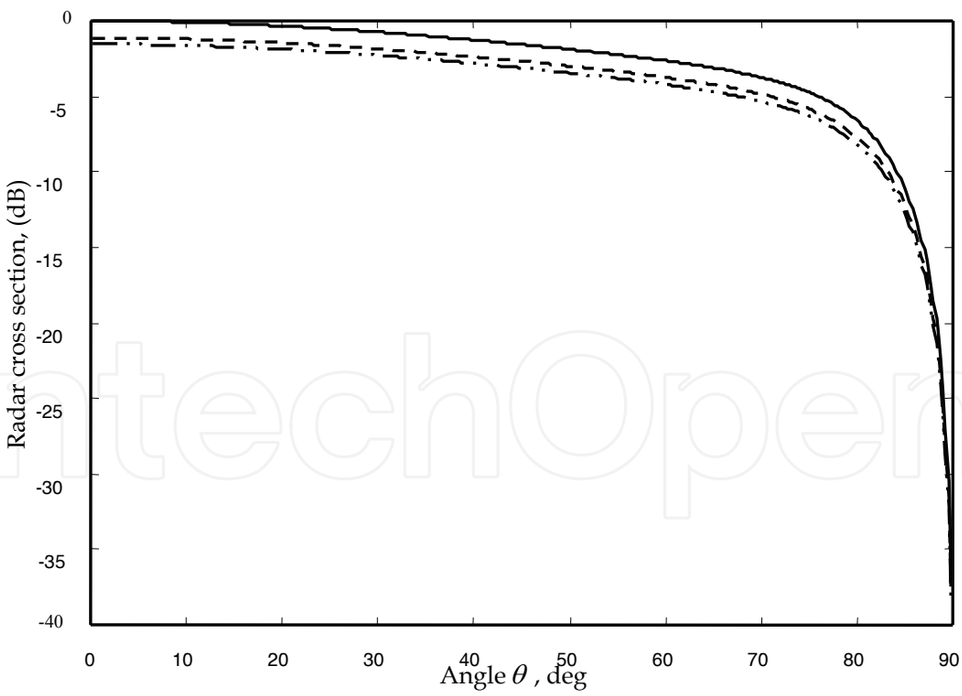

(b) ε_x changed, ——— $\varepsilon_x = \varepsilon_z = 5$, - - - - $\varepsilon_x = 3.6$, $\varepsilon_z = 5$, — · · — $\varepsilon_x = 6.4$, $\varepsilon_z = 5$.

Fig. 3. Normalized radar cross section versus angle θ for the isotropic, positive uniaxial anisotropic and negative uniaxial anisotropic substrates.

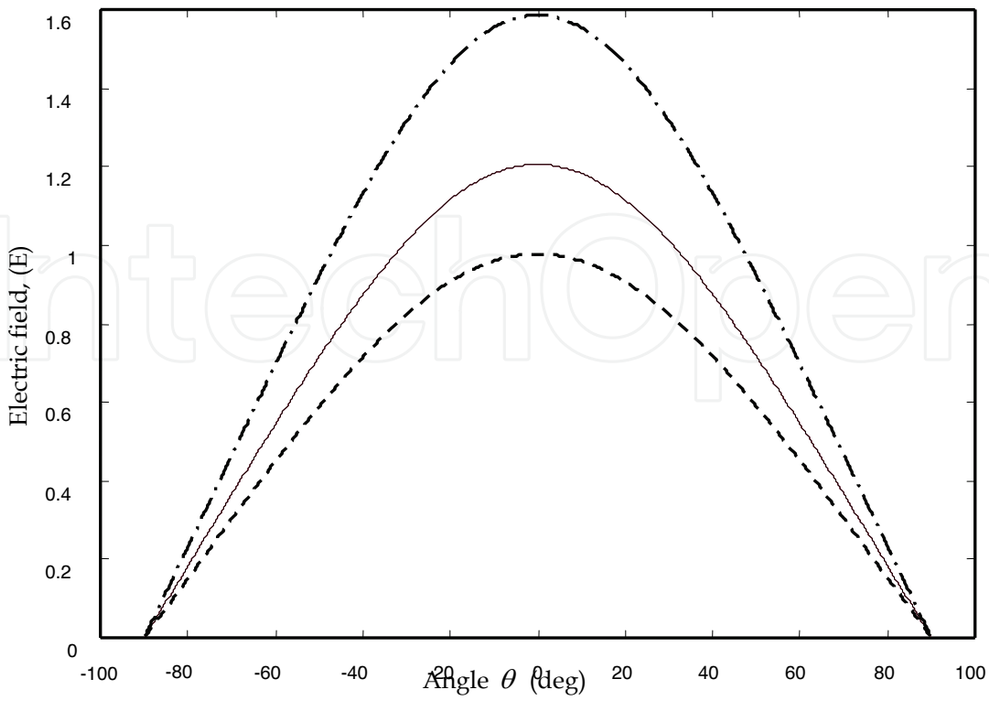

(a) ε_z changed, ——— $\varepsilon_x = \varepsilon_z = 5$, – – – – $\varepsilon_x = 5, \varepsilon_z = 6.4$, — · — · $\varepsilon_x = 5, \varepsilon_z = 3.6$

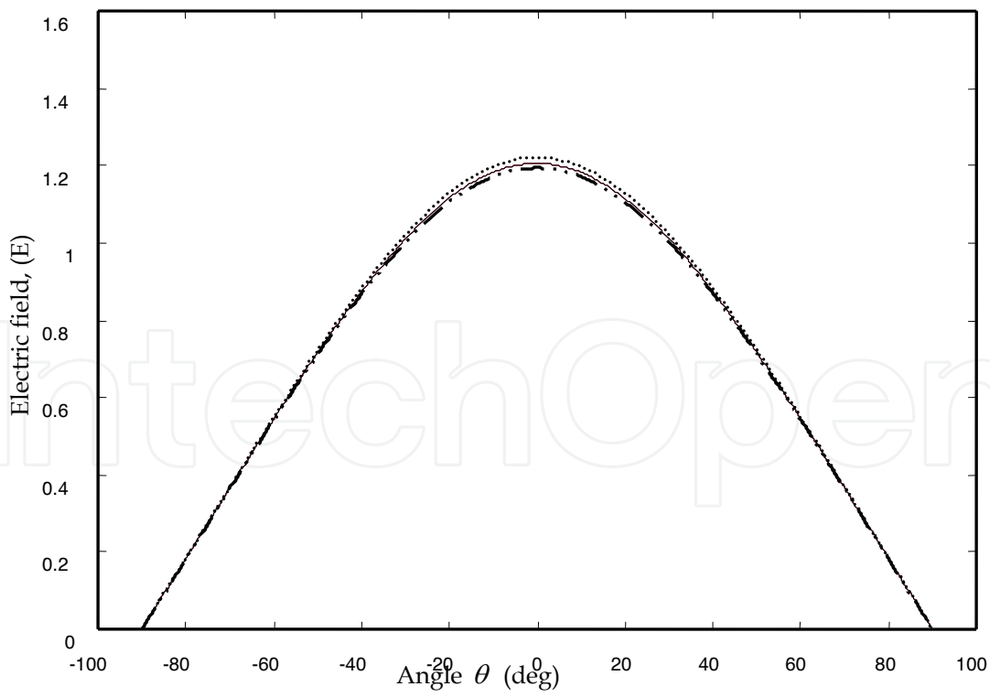

(b) ε_x changed, ——— $\varepsilon_x = \varepsilon_z = 5$, ····· $\varepsilon_x = 3.6,\ \varepsilon_z = 5$, — · · — $\varepsilon_x = 6.4,\ \varepsilon_z = 5$.

Fig. 4. Radiation pattern versus the angle θ for the isotropic, positive uniaxial anisotropic and negative uniaxial anisotropic substrates.

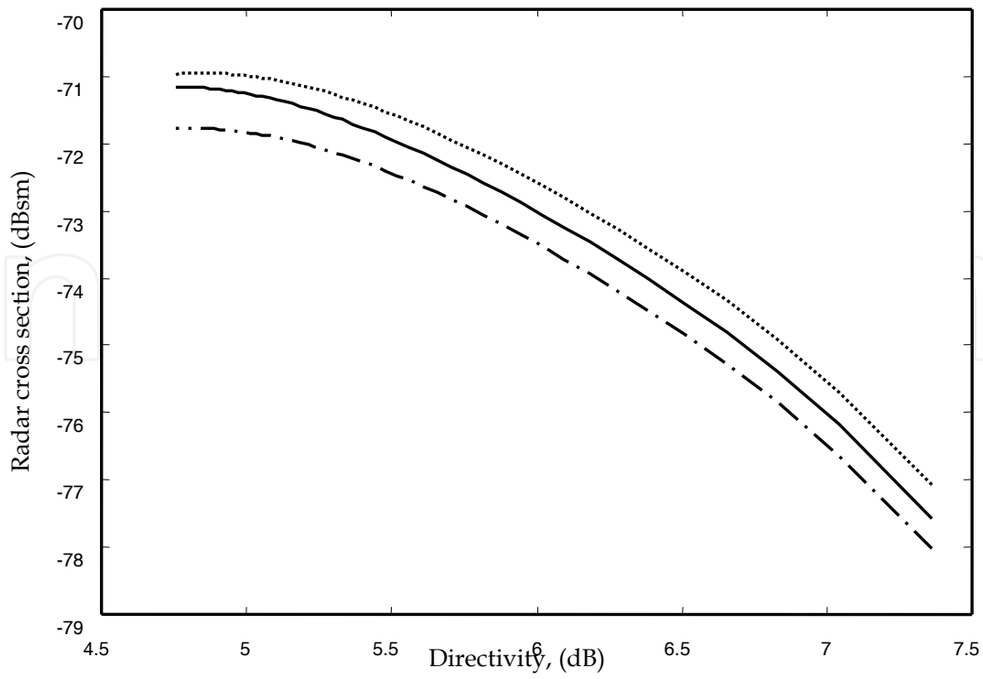

(a) ε_z changed, ——— $\varepsilon_x = \varepsilon_z = 5$, — · — $\varepsilon_x = 5$, $\varepsilon_z = 6.4$, ····· $\varepsilon_x = 5$, $\varepsilon_z = 3.6$.

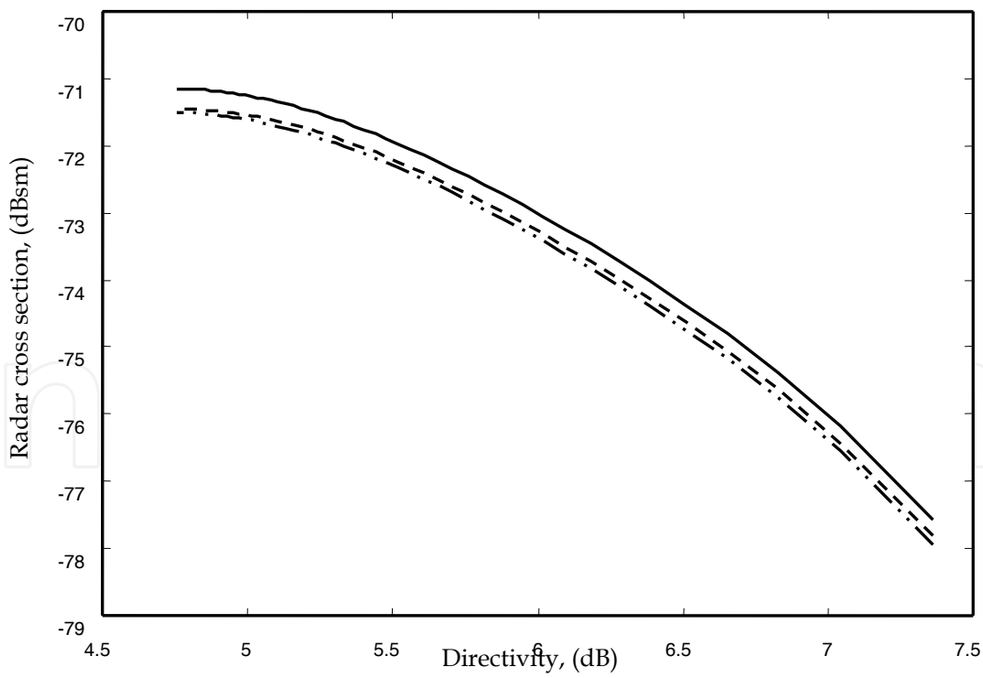

(b) ε_x changed, ——— $\varepsilon_x = \varepsilon_z = 5$, - - - - $\varepsilon_x = 3.6, \varepsilon_z = 5$, — · · — $\varepsilon_x = 6.4$, $\varepsilon_z = 5$.

Fig. 5. Radar cross section versus the directivity for the isotropic, positive uniaxial anisotropic and negative uniaxial anisotropic substrates.

Figures 3 and 4 show the influence of uniaxial anisotropy in the substrate on the radiation and the radar cross section displayed as a function of the angle θ at $\varphi = 0°$ plane and at the frequency 5.95 Ghz, where the isotropic($\varepsilon_z = \varepsilon_x$), positive uniaxial anisotropic ($\varepsilon_z > \varepsilon_x$) and negative uniaxial anisotropic substrates ($\varepsilon_z < \varepsilon_x$) are considered, a rectangular patch antenna with dimensions *a*=1.5cm, *b*=1.0 cm is embedded in a single substrate with thickness *h*=0.2 cm. The obtained results can be seen to be the same as discussed previously in the case of the resonant frequency, moreover the permittivity ε_z along the optical axis is the most important factor in determining the resonant frequency, the radiation and the radar cross section when the pair (ε_x , ε_z) changes.
The same remarks hold for the variation of the radar cross section versus the directivity figures (5. a, b).
It is worth noting that the radar cross section in equation (39) is calculated at one frequency. If one needs the radar cross section over a frequency range, this calculation must be repeated for the different frequencies of interest.

4. Conclusion

The moment method technique has been developed to examine the resonant frequency, the radiation, the half power band width, the directivity and the scattering radar cross section of a rectangular microstrip patch antenna. The boundary condition for the electric field was used to derive an integral equation for the electric current, the Galerkin's procedure of the moment method with entire domain sinusoidal basis functions without edge condition was investigated, the resulting system of equations was solved for the unknown current modes on the patch, it is important to note that the dyadic Green's functions of the problem were efficiently determined by the (TM, TE) representation. Since there has been a little work on the scattering radar cross section of patch antennas including the effect of uniaxial anisotropic substrate in the literature, a number of results pertaining to this case were presented in this chapter. The obtained results show that the use of the uniaxial anisotropy substrates significantly affects the characterization of the microstrip patch antennas. The numerical results indicate that the resonant frequency and the half power band width are increased due to the positive uniaxial anisotropy when ε_x change, on the other hand, decreased due to the negative uniaxial anisotropy. Moreover the ε_z permittivity has a stronger effect on the resonant frequency, the radiation and the radar cross section than the permittivity ε_x . Also the effect of the uniaxial substrate on the radar cross section versus the directivity was presented. Accuracy of the computed techniques presented and verified with other calculated results.
A new approach for enhancement circular polarisation output in the rectangular patch antenna based on the formulation presented in this chapter is in progress and will be the subject of a future work, when two chamfer cuts will be used to create the right or the left handed circular polarisation by exciting simultaneously two nearly degenerate patch modes. The analysis presented here can also be extanded to study a biaxially anisotropic substrate and the effect of dielectric cover required for the protection of the antenna from the environment. Also the radar cross section monostatic and bistatic and the other antenna characteristics will be study for this case in our future work.

5. References

Bhartia, P.; Rao, K. V. S.& Tomar, R. S. (1991). *Millimeter Wave Microstrip and Printed Circuit Antennas*, Publisher, Artech House, ISBN 0-89006-333-8, Boston, London

Boufrioua, A. & Benghalia, A. (2008). Radiation and resonant frequency of a resistive patch and uniaxial anisotropic substrate with entire domain and roof top functions, *Elsevier, EABE, Engineering Analysis with Boundary Elements*, Vol., 32, No. 7, (March 2008), (591-596), ISSN 0955-7997

Boufrioua, A. (2009). Resistive Rectangular Patch Antenna with Uniaxial Substrate. In: *Antennas: Parameters, Models and Applications* (Ed. Albert I. Ferrero), (163-190), Publisher, Nova, ISBN 978-1-60692-463-1, New York

Bouttout, F.; Benabdelaziz, F.; Benghalia, A.; Khedrouche, D. & Fortaki, T. (1999), Uniaxially Anisotropic Substrate Effects on Resonance of Rectangular Microstrip Patch Antenna, *Electronics Letters*, Vol. 35, No. 4, (February 1999), (255-256), ISSN 0013-5194

Chew, W. C. & Liu, Q. (1988), Resonance Frequency of a Rectangular Microstrip Patch, *IEEE Transactions on Antennas and Propagation*, Vol. 36, No. 8, (August 1988), (1045-1056), ISSN 0018-926X

Damiano, J. P. & Papiernik, A. (1994), Survey of Analytical and Numerical Models for Probe-Fed Microstrip Antennas, *IEE proceeding. Microwaves, Antennas and Propagation*, Vol. 141, No. 1, (February 1994), (15-22), ISSN 1350-2417

Knott, E. F.; Shaeffer, J. F. & Tuley, M. T. (2004). *Radar Cross Section*, Publisher SciTech, ISBN 1-891121-25-1, Raleigh, NC

Mirshekar-Syahkal, D. (1990). *Spectral Domain Method for Microwave Integrated Circuits*, Publisher, John Wiley & Sons Inc, ISBN 0-86380-099-8, New York

Newman, E. H. & Forrai, D. (1987). Scattering from a Microstrip Patch, *IEEE Transactions on Antennas and Propagation*, Vol. 35, No. 3, (March 1987), (245-251) ISSN 0018-926X

Pozar, D. M. (1987). Radiation and Scattering from a Microstrip Patch on a Uniaxial Substrate, *IEEE Transactions on Antennas and Propagation*, Vol. 35, No. 6, (June 1987), (613-621), ISSN 0018-926X

Pozar, D. M. & Voda, S. M. (1987). A Rigorous Analysis of a Microstripline Fed Patch Antenna, *IEEE Transactions on Antennas and Propagation*, Vol. 35, No. 12, (December 1987), (1343-1350), ISSN 0018-926X

Reddy, V. M.; Deshpand, D.; Cockrell, C. R. & Beck, F. B. (1998). Fast RCS Computation Over a Frequency Band Using Method of Moments in Conjuction with Asymptotic Waveform Evaluation Technique, *IEEE Transactions on Antennas and Propagation,* Vol. 46, No. 8, (August 1998), (1229-1233), ISSN 0018-926X

Row, J. S. & Wong, K. L. (1993). Resonance in a Superstrate-Loaded Rectangular Microstrip Structure, *IEEE Transactions on Antennas and Propagation*, Vol. 41, No. 8, (August 1993), (1349-1355), ISSN 0018-9480

Tulintsef, A. N.; Ali, S. M. & Kong, J. A. (1991). Input Impedance of a Probe-Fed Stacked Circular Microstrip Antenna, *IEEE Transactions on Antennas and Propagation*, Vol. 39, No. 3, (March 1991), (381-390), ISSN 0018-926X

Wong, K. L.; Row, J. S.; Kuo, C. W. & Huang, K. C. (1993). Resonance of a Rectangular Microstrip Patch on a Uniaxial Substrate, *IEEE Transactions on Microwave Theory and Techniques*, Vol., 41 No. 4, (April 1993), (698-701), ISSN 0018-9480

Microstrip Antennas

Edited by Prof. Nasimuddin Nasimuddin

ISBN 978-953-307-247-0
Hard cover, 540 pages
Publisher InTech
Published online 04, April, 2011
Published in print edition April, 2011

In the last 40 years, the microstrip antenna has been developed for many communication systems such as radars, sensors, wireless, satellite, broadcasting, ultra-wideband, radio frequency identifications (RFIDs), reader devices etc. The progress in modern wireless communication systems has dramatically increased the demand for microstrip antennas. In this book some recent advances in microstrip antennas are presented.

InTech Europe
University Campus STeP Ri
Slavka Krautzeka 83/A
51000 Rijeka, Croatia
Phone: +385 (51) 770 447
Fax: +385 (51) 686 166
www.intechopen.com

InTech China
Unit 405, Office Block, Hotel Equatorial Shanghai
No.65, Yan An Road (West), Shanghai, 200040, China
中国上海市延安西路65号上海国际贵都大饭店办公楼405单元
Phone: +86-21-62489820
Fax: +86-21-62489821

IntechOpen